DOI: 10.1002/zaac.200900447

Synthesis, Crystal Structure and Vibrational Spectra of Barium Cyclotetraphosphate Hydrate $Ba_2(P_4O_{12})\cdot 3.5H_2O$

Henning A. Höppe,*[a] Karolina Kazmierczak,[a] and Michael Daub[a]

Keywords: Structure elucidation; Barium; Phosphates; Vibrational spectroscopy; Thermal analysis

Abstract. Barium tetrametaphosphate hydrate $Ba_2(P_4O_{12})\cdot 3.5H_2O$ was synthesized as a single-phase crystalline powder starting from an aqueous solution of barium hydroxide and phosphorus pentoxide at 300 K. $Ba_2(P_4O_{12})\cdot 3.5H_2O$ crystallizes in a new structure type in which the Ba^{2+} ions form a distorted hexagonal diamond-like arrangement with the $(P_4O_{12})^{4-}$ anions in the trigonal prismatic voids ($Ba_2(P_4O_{12})\cdot 3.5H_2O$, *C*2/*c*, *Z* = 4, *a* = 777.3(2), *b* = 1297.6(2), *c* = 1346.1(3) pm, *b* = 95.38(2)°, wR_2 = 0.071, R_1 = 0.018, 1180 reflections, 118 parameters). The vibrational spectra of $Ba_2(P_4O_{12})\cdot 3.5H_2O$ and its thermal behavior up to 720 K are also reported.

Introduction

During our systematic search for precursor compounds for the low-temperature synthesis of condensed alkaline earth phosphates like two polymorphs of $BaHPO_4$ [1] we discovered the new cyclotetraphosphate hydrate $Ba_2(P_4O_{12})\cdot 3.5H_2O$. An indexed powder diffraction pattern of a compound of similar composition was already given [2] which can now be attributed to this cyclotetraphosphate. The targeted alkaline earth phosphates attract interest in materials science due to the possibility of doping them with divalent or trivalent rare earth ions to produce efficient fluorescent materials [3].So far, of the alkaline earth cyclotetraphosphates only $Ca_2(P_4O_{12})\cdot 4H_2O$ [4] and strontium cyclotetraphosphate $Sr_2(P_4O_{12})\cdot 6H_2O$ [5] have been successfully characterized. In this contribution the solution of the crystal structure of the possible precursor compound for condensed barium phosphates $Ba_2(PO_3)_4\cdot 3.5H_2O$ including a thermogravimetric study will be presented. Additionally, the vibrational spectra of $Ba_2(PO_3)_4\cdot 3.5H_2O$ are reported.

Results and Discussion

1. Crystal Structure

The crystal structure of $Ba_2(P_4O_{12})\cdot 3.5H_2O$ comprises non-condensed cyclotetraphosphate (tetrametaphosphate) anions coordinating the embedded barium ions and crystal water molecules.

The barium atoms in the new structure type of $Ba_2(P_4O_{12})\cdot 3.5H_2O$ form a distorted hexagonal diamond like substructure with Ba–Ba distances between 435 and 470 pm within the corrugated chair layers running perpendicular [001]. These are linked along [001] with Ba–Ba distances of 583 pm (Table 3) forming six-rings with boat conformation (Figure 1). Between the barium sheets perpendicular [001] almost trigonal prismatic voids are located at 0/½/¼ (void 1), 0/0.1667/¼ (void 2) and 0/0.8333/¼ (void 3). This follows from the direct group-subgroup symmetry relations starting from hexagonal diamond (Figure 2). These voids are occupied by the tetrametaphosphate ions (void 1), the crystal water molecules OW2 (void 2) and OW1 (void 3) as shown in Figure 1.

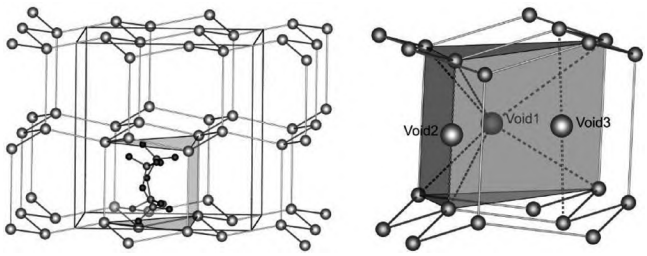

Figure 1. Perspective view the unit cell of $Ba_2(P_4O_{12})\cdot 3.5H_2O$ approximately along [100], the lines connecting the grey barium atoms visualize their diamond-like arrangement and do not represent bonds in a chemical sense; a trigonal prismatic void filled with a cyclotetraphosphate anion is shown as translucent polyhedron (left); all three voids viewed along [120] (right).

In calcium cyclotetraphosphate tetrahydrate, $Ca_2(P_4O_{12})\cdot 4H_2O$ [4], the calcium ions form an arrangement similar to cubic diamond, and therefore $Ca_2(P_4O_{12})\cdot 4H_2O$ has an unit cell with less than a half of the *c* axis found in the barium compound.

Figure 3 gives an overview about the unit cell of $Ba_2(P_4O_{12})\cdot 3.5H_2O$ including the crystal water molecules which are located in the remaining voids of the structure.

* Dr. H. A. Höppe
Fax: +49-761-203-6012
E-Mail: henning.hoeppe@ac.uni-freiburg.de
[a] Institut für Anorganische und Analytische Chemie
Albert-Ludwigs-Universität Freiburg
Albertstr. 21
79104 Freiburg im Breisgau, Germany
Supporting information for this article is available on the WWW under **http://dx.doi.org/10.1002/zaac.200900447** or from the author.

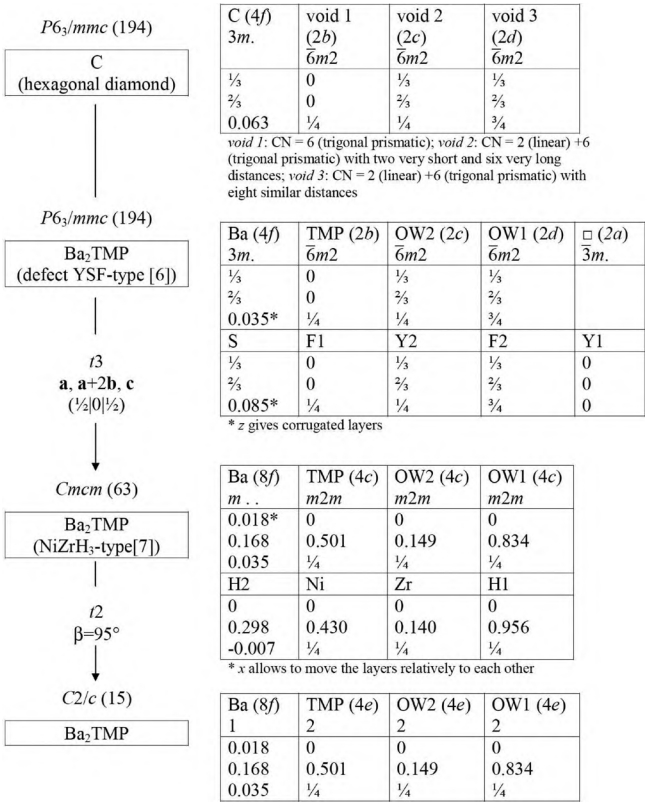

C (4*f*) 3*m*.	void 1 (2*b*) $\bar{6}m2$	void 2 (2*c*) $\bar{6}m2$	void 3 (2*d*) $\bar{6}m2$
⅓	0	⅓	⅓
⅔	0	⅔	⅔
0.063	¼	¼	¾

void 1: CN = 6 (trigonal prismatic); *void 2*: CN = 2 (linear) +6 (trigonal prismatic) with two very short and six very long distances; *void 3*: CN = 2 (linear) +6 (trigonal prismatic) with eight similar distances

Ba (4*f*) 3*m*.	TMP (2*b*) $\bar{6}m2$	OW2 (2*c*) $\bar{6}m2$	OW1 (2*d*) $\bar{6}m2$	□ (2*a*) $\bar{3}m$.
⅓	0	⅓	⅓	
⅔	0	⅔	⅔	
0.035*	¼	¼	¾	
S	F1	Y2	F2	Y1
⅓	0	⅓	⅓	0
⅔	0	⅔	⅔	0
0.085*	¼	¼	¾	0

* *z* gives corrugated layers

Ba (8*f*) *m* . .	TMP (4*c*) *m2m*	OW2 (4*c*) *m2m*	OW1 (4*c*) *m2m*
0.018*	0	0	0
0.168	0.501	0.149	0.834
0.035	¼	¼	¼
H2	Ni	Zr	H1
0	0	0	0
0.298	0.430	0.140	0.956
-0.007	¼	¼	¼

* *x* allows to move the layers relatively to each other

Ba (8*f*) 1	TMP (4*e*) 2	OW2 (4*e*) 2	OW1 (4*e*) 2
0.018	0	0	0
0.168	0.501	0.149	0.834
0.035	¼	¼	¼

Figure 2. Group-subgroup scheme visualizing the relationship between the cationic arrangement including filling of the voids in $Ba_2(P_4O_{12})\cdot 3.5H_2O$ and the crystal structure of hexagonal diamond.

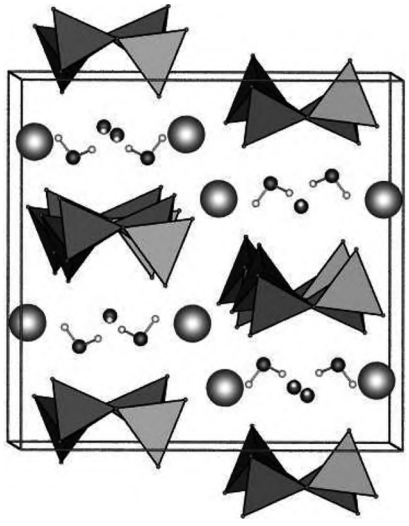

Figure 3. Unit cell of $Ba_2(P_4O_{12})\cdot 3.5H_2O$ viewed approximately along [100].

The cyclotetraphosphate anion exhibits C_2 symmetry (Figure 4), the bond lengths between the phosphorus and the terminal O^{term} atoms ranging from 148.1(2) to 148.4(2) pm (average 148.3 pm) are shorter than the bond lengths between the phosphorus and the bridging O^{br} atoms [160.1(2) and 161.2(2) pm, average 160.6 pm]. They agree well with typical bond lengths inside phosphate chains in *catena*-phosphates [8]. As observed previously in *catena*- or cyclophosphates, the angles O^{br}–P–O^{br} [102.9(1)° and 102.2(1)°] are significantly smaller compared with the angles O^{term}–P–O^{term} [116.5(2)° and 120.5(2)°] due to a partial double-bond character of the P–O^{term} bonds.

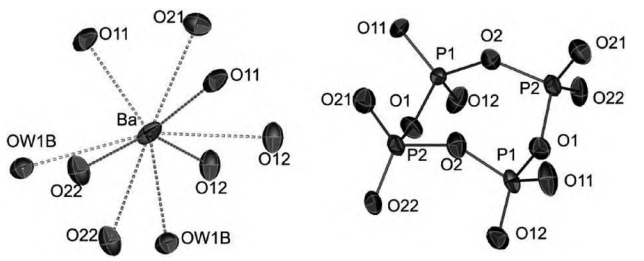

Figure 4. Representation of the coordination environment of the barium atoms (left) and of the cyclotetraphosphate anion (right) in $Ba_2(P_4O_{12})\cdot 3.5H_2O$, all displacement ellipsoids are drawn on a probability level of 75 %.

The deviation of the PO_4 tetrahedra from ideal symmetry was calculated applying the method of all ligands enclosing spheres on experimental data. In this method not only distance variations inside a polyhedron are considered but also angle deviations caused by larger distortions. In a first step the optimum centroid of the four surrounding oxygen atoms, i.e. the phosphorus atom, is determined by a least-squares refinement [9] and gives a medium centroid-ligand distance r_{centr}. Subsequently, the volume of an ideal tetrahedron given by Equation 1a is calculated using r_{centr}. Finally, this volume is compared with the volume of the experimentally obtained body built up by four vertices [10]. This volume can be calculated using Equation 1b

$$\frac{8r_{centr}^3}{9\sqrt{3}} \quad (1a)$$

$$\frac{S\cdot h}{3} \quad (1b)$$

where S is the base area built from three vertices and h is the height of the body obtained by the distance of the fourth vertex from the base. The two crystallographically different PO_4 tetrahedra in $Ba_2(P_4O_{12})\cdot 3.5H_2O$ feature the values 0.14 % (P1) and 0.42 % (P2). These values are typical for phosphate tetrahedra found in the recent literature and confirm the consistency of our structure model. In general, the deviations in condensed phosphates ought to be larger compared with those of non-condensed orthophosphates due to the different bonding situations of terminal and bridging oxygen atoms which is the case. In orthophosphates the deviation is close to 0 %, e.g. for Li_3PO_4 [11] we calculated a deviation of 0.01 %.

The Ba^{2+} ions are coordinated by seven terminal oxygen atoms of the tetracyclophosphate anion and two oxygen atoms of crystal water molecules (Figure 4), the distances Ba–O vary between 261.6(5) and 293.5(2) pm with an average value of 282.8 pm in very good agreement with the sum of ionic radii of 280 pm [12].

Figure S1 (supplementary material) shows the hydrogen bonds found in $Ba_2(P_4O_{12})\cdot 3.5H_2O$. According to hydrogen bond schemes [13] the strength of these can be classified as moderate. An overview of the hydrogen bonds determined in $Ba_2(P_4O_{12})\cdot 3.5H_2O$ is given in Table 4.

Further details of the crystal structure investigations may be obtained from the Fachinformationszentrum Karlsruhe, Abt. PROKA, 76344 Eggenstein-Leopoldshafen, Germany (E-Mail: crysdata@fiz-karlsruhe.de) on quoting the depository number CSD-420500, the name of the authors and citation of this publication.

2. Thermal Analysis

According to the thermogravimetric data our sample of $Ba_2(P_4O_{12})\cdot 3.5H_2O$ shows a total weight loss of 8.2 weight-% (theoretical value: 9.6 weight-%) during heating from room temperature to 720 K (Figure 5). Due to calibration process the sample lost already 0.8 % during the start of the measurement. Between room temperature and 420 K the mass loss amounts to 6.3 weight-% (5.5 %+0.8 %) already which would correspond with 2.5 crystal water molecules per formula unit. The remaining crystal water is probably lost between 420 K and 650 K. Since P_4O_{10} sublimes also in this temperature range we cannot exclude an additional phosphate loss. Moreover, the nature of the amorphous parts of our sample is not known in detail, and therefore we attribute the difference between theoretical and determined values to the amorphous parts of our sample.

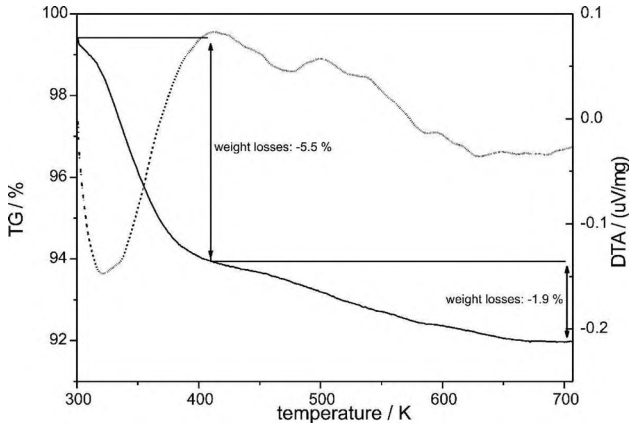

Figure 5. DTA/TG data of $Ba_2(P_4O_{12})\cdot 3.5H_2O$ in the range from room temperature to 720 K.

Our data are basically in agreement with previous data on the thermal degradation of other hydrated barium phosphates [14]. In contrast to this previous work, we observed barium polyphosphate [15] as single crystalline phase present in the rather amorphous decomposition product (supplementary material Figure S2).

3. Vibrational Spectroscopy

Figure 6 shows the IR and Raman spectra of the title compound $Ba_2(P_4O_{12})\cdot 3.5H_2O$. The IR spectra of *catena*-polyphosphates are significantly different from those of orthophosphates [16]. The only characteristic bands should be found in the region between 800 and 650 cm^{-1}, where the number of signals should match with the periodicity of the phosphate chain. This is clearly the case as two bands are found in this area for $Ba_2(P_4O_{12})\cdot 3.5H_2O$ corresponding to the two crystallographically independent phosphorus atoms.

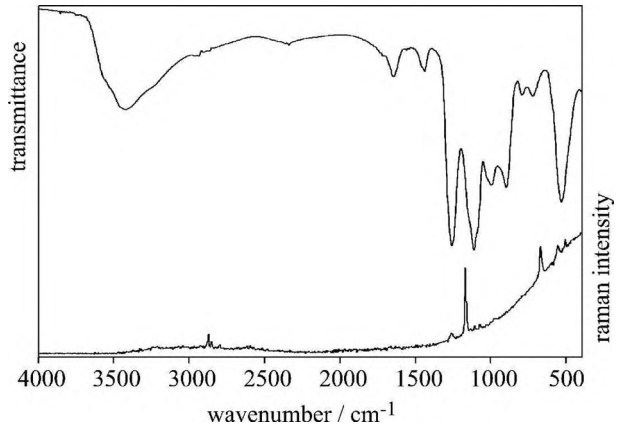

Figure 6. Vibrational spectra of $Ba_2(PO_3)_4\cdot 3.5H_2O$.

The strongest bands in $Ba_2(P_4O_{12})\cdot 3.5H_2O$ can be assigned to $\nu(PO^{term})$ and $\nu_{as}(PO_2)$ vibrations and range from 1195 to 950 cm^{-1} and from 1320 to 1195 cm^{-1}, respectively. The $\nu_{as}(POP)$ vibration recorded at 895 cm^{-1} is significantly shifted to lower wavenumbers compared with other not strained poly- and oligophosphates where this band is found around 940 cm^{-1} [8]. Additionally, rather intense H–O vibrations are found with a maximum at 3425 cm^{-1} typical for moderately strong hydrogen bonds [13]. The $\delta(H_2O)$ vibration is detected at 1645 cm^{-1}.

Additionally, the Raman spectra of $Ba_2(P_4O_{12})\cdot 3.5H_2O$ show strong vibrations in the region around 1175 [$\nu_s(PO_2)$], and at 675 cm^{-1} [$\nu_s(POP)$]. Thus, the observed vibrational data are in very good agreement with the expected values.

Experimental Section

1. Synthesis

The synthesis of $Ba_2(P_4O_{12})\cdot 3.5H_2O$ was performed in a Petri dish according to Equation 2.

$$4\ Ba(OH)_2 + 2\ P_4O_{10} + 3\ H_2O \rightarrow 2\ Ba_2(P_4O_{12})\cdot 3.5H_2O \qquad (2)$$

Barium hydroxide $Ba(OH)_2$ (51.3 mg, 0.294 mmol; Merck, pure) was dissolved in a Petri dish with water (10 mL). Afterwards, phosphorus pentoxide P_2O_5 (23.0 mg, 0.162 mmol; Roth, 98.5 %) was added to the solution. The covered Petri dish was allowed to dry at 300 K until the water was almost evaporated (2 d). The reaction yielded a colorless and non-hygroscopic powder of $Ba_2(P_4O_{12})\cdot 3.5H_2O$ containing single-crystals, which could be easily separated from the remaining liquid.

2.1 Crystal Structure Determination

A suitable single-crystal of $Ba_2(P_4O_{12})\cdot 3.5H_2O$ was enclosed in a glass capillary. X-ray diffraction data were collected with a Bruker AXS CCD diffractometer fitted with an APEX-II detector and corrected for absorption by applying a multi-scan correction. The diffraction pattern was indexed on the basis of a *C*-centered monoclinic unit cell. The crystal structure of $Ba_2(P_4O_{12})\cdot 3.5H_2O$ was solved by direct methods using SHELXTL [17] in space group *C*2/*c* (no. 15) and refined with anisotropic displacement parameters for all non-hydrogen atoms. The hydrogen atoms could be localized by difference Fourier syntheses. To maintain reasonable distances to the oxygen atoms the O–H distances were commonly refined giving an average O–H distance of 91(2) pm. The crystal water molecules were found to be split over two positions each indicated as A and B position, respectively, with refined fractional occupation factors around 0.5.

The relevant crystallographic data and further details of the X-ray data collection are summarized in Table 1. Table 2 shows the positional and displacement parameters for all atoms. In Table 3 selected interatomic distances and angles are listed, Table 4 contains information about the hydrogen bonds found in $Ba_2(P_4O_{12})\cdot 3.5H_2O$.

Table 1. Crystallographic data of $Ba_2(P_4O_{12})\cdot 3.5H_2O$ (estimated standard deviations in parentheses).

Crystal Data	
$Ba_2(P_4O_{12})\cdot 3.5H_2O$	$F(000) = 1212$
$M = 653.62$ g·mol^{-1}	$\rho_{X-ray} = 3.212$ g·cm^{-3}
monoclinic	Mo-K_α radiation
space group *C*2/*c* (no. 15)	$\lambda = 0.71073$ Å
$a = 7.773(2)$ Å	
$b = 12.976(2)$ Å	$\beta = 95.38(2)°$
$c = 13.461(3)$ Å	crystal shape: plate
$V = 1351.7(4)$ Å^3	0.02 × 0.08 × 0.10 mm
$Z = 4$	colorless
$\mu = 6.35$ mm^{-1}	$T = 293(2)$ K
Data Collection	
Bruker AXS CCD APEX II	
absorption corr.: multi-scan	$h = -9 \rightarrow 9$
$T_{min} = 0.5802$; $T_{max} = 0.8801$	$k = -15 \rightarrow 15$
$R_{int} = 0.027$; $R_\sigma = 0.083$	$l = -16 \rightarrow 16$
$2\theta_{max} = 50.0°$	
1180 independent reflections, 1154 obs. refl. ($F_o^2 \geq 2\,\sigma\,(F_o^2)$)	
Refinement	
refinement on F^2	
program used to refine structure: SHELXL-97 [17]	
$R1 = 0.018$	
$w^{-1} = \sigma^2 F_o^2 + (xP)^2 + yP$; $P = (F_o^2 + 2F_c^2)/3$, $x = 0$, $y = 0$	
$wR2 = 0.071$	
GooF = 0.885	
118 parameters, 16 restraints (distances O–H, adp./occ. OW)	
maximal/minimal residual electron density: 0.75/–0.61 e·Å^{-3}	
Powder Diffraction (Rietveld refinement)	
$Ba_2(PO_3)_4\cdot 3.5H_2O$	Mo-K_α radiation
program used: GSAS [18]	$wR_P = 0.035$
$a = 7.7880(4)$ Å	$R_P = 0.027$
$b = 13.0069(7)$ Å	$\beta = 95.343(5)°$
$c = 13.4761(7)$ Å	$R_F = 0.070$
$R_F2 = 0.123$	$\chi^2 = 4.55$
refined parameters: 12	
639 reflections ($2\theta_{max} = 40.0°$)	

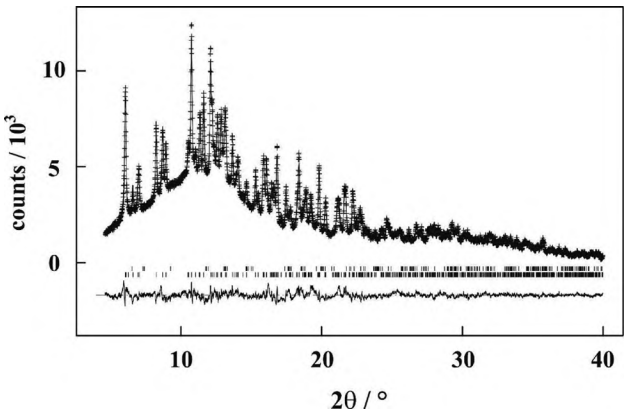

Figure 7. Observed (crosses) and calculated (line) X-ray powder diffraction pattern (Mo-K_α radiation) as well as the difference profile of the Rietveld refinement of $Ba_2(P_4O_{12})\cdot 3.5H_2O$. The upper row of vertical lines indicate possible peak positions of $Ba_2(P_4O_{12})\cdot 3.5H_2O$, the bottom row gives possible peak positions of the simultaneously refined SiO_2 (coesite).

2.2 Rietveld Refinement

A sample of $Ba_2(P_4O_{12})\cdot 3.5H_2O$ was enclosed in a glass capillary with 0.2 mm diameter and investigated at room temperature in Debye–Scherrer geometry on a STOE Stadi P powder diffractometer with Ge(111)–monochromatized Mo-K_α radiation (linear PSD detector, step width 0.5°). The powder diffraction pattern of the raw product presented in Figure 1 shows amorphous contributions and minor contributions of coesite (SiO_2) from the handling in the mortar. To confirm the refined structure model and to check the phase purity of the title compound a Rietveld refinement was performed. All reflections detected by X-ray powder diffraction of $Ba_2(P_4O_{12})\cdot 3.5H_2O$ have been indexed and their observed intensities are in very good agreement with the calculated diffraction pattern based on the single crystal data as well as the powder diffraction pattern deposited in the powder diffraction file 43–517 [2]. The Rietveld refinement of the structure model (Figure 7, Table 1) has been performed with the program GSAS [18] and confirms the single crystal data. The atomic parameters remain almost unchanged and therefore the detailed structural parameters are not reproduced herein.

3. Thermal Analysis

Thermogravimetric analyses were carried out on a sample of sorted single-crystals of $Ba_2(P_4O_{12})\cdot 3.5H_2O$ in an alumina sample holder using a simultaneous thermoanalysis apparatus STA409 from Netzsch under air (heating rate: 1 K·min^{-1}, flow-rate: 75 mL·min^{-1}) in the range from room temperature to 720 K.

4. Vibrational Spectroscopy

An FTIR spectrum was obtained at room temperature by using a Bruker IFS 66v/S spectrometer. The samples were thoroughly mixed with dried KBr (approx. 2 mg sample, 300 mg KBr). Raman spectra were recorded by a Bruker FRA 106/S module with a Nd–YAG laser ($\lambda = 1064$ nm) scanning a range from 400 to 4000 cm^{-1}.

Supporting Information (see footnote on the first page of this article): Figures showing the hydrogen bonds in the title compound (S1) and the powder diffractogram of the decomposition product (S2).

atom	f. o. f.	x	y	z	U_{11}	U_{22}	U_{33}	U_{23}	U_{13}	U_{12}	U_{eq}/U_{iso}
Ba	1	0.48122(2)	0.33181(2)	0.96529(2)	180(2)	197(2)	194(2)	920(5)	1082(13)	1083(6)	184(2)
P1	1	0.79323(9)	0.41694(5)	0.14228(5)	134(4)	127(4)	135(4)	27(2)	53(3)	46(3)	129(2)
P2	1	0.16462(9)	0.45109(6)	0.13459(5)	148(4)	158(4)	125(4)	–4(3)	59(3)	00(3)	141(2)
O1	1	0.7972(3)	0.3942(2)	0.2596(2)	205(10)	180(10)	133(9)	7(7)	51(8)	–15(8)	171(4)
O2	1	0.9649(3)	0.4840(2)	0.1363(2)	172(11)	168(10)	202(10)	39(8)	66(8)	14(8)	178(4)
O12	1	0.8075(3)	0.3156(2)	0.0930(2)	152(12)	247(12)	196(11)	–55(8)	6(10)	57(9)	199(5)
O21	1	0.2599(3)	0.5497(2)	0.1319(2)	223(12)	209(11)	210(10)	8(8)	71(9)	–26(9)	211(5)
O22	1	0.1848(3)	0.3704(2)	0.0584(2)	136(11)	308(12)	162(10)	–50(9)	57(8)	–6(9)	199(5)
O11	1	0.6416(3)	0.4811(2)	0.1070(2)	172(12)	214(11)	293(12)	112(8)	93(9)	108(9)	222(5)
OW1A	0.499(4)	0.5158(6)	0.2213(3)	0.1529(3)	179(14)	164(16)	181(14)	35(11)	50(14)	28(13)	173(6)
OW1B	0.501(4)	0.3926(5)	0.2095(3)	0.1344(3)	179(14)	164(16)	181(14)	35(11)	50(14)	28(13)	173(6)
OW2A	0.503(3)	½	0.3512(5)	¾	145(19)	22(2)	171(18)	0	00(15)	0	178(8)
OW2B	0.497(3)	0.3068(6)	0.3252(3)	0.7895(4)	145(19)	22(2)	171(18)	0	00(15)	0	178(8)
H11	1	0.4762(10)	0.168(2)	0.113(3)							30
H12	1	0.433(5)	0.198(3)	0.199(2)							30
H21	1	0.383(2)	0.343(3)	0.745(3)							30
H22	0.50	0.293(10)	0.2561(15)	0.780(5)							30

Table 3. Selected interatomic distances /pm and angles /° for $Ba_2(P_4O_{12})\cdot 3.5H_2O$ (estimated standard deviations in parentheses).

Ba–O		261.6(5)–293.5(2)	9 distances
Ba–Ba		435.09(7), 446,78(7), 470.19(8), 583.1(1)	
P–O^{br}		160.1(2)–161.2(2)	Ø = 160.6
P–O^{term}		148.1(2)–148.4(2)	Ø = 148.3
O^{br}–P–O^{br}	102.0(1), 102.2(1)	Ø = 102.1	
O^{term}–P–O^{term}	116.5(2), 120.5(2)	Ø = 118.5	

Table 4. Hydrogen bonds in $Ba_2(P_4O_{12})\cdot 3.5H_2O$; D = donor, A = acceptor; all distances are given in pm, angles in °.

D–H	d(D–H)	d(H–A)	∠(DHA)	d(D–A)	A
OW1A–H11	91	242	133	311	O2
OW1A–H11	91	257	142	333	O22
OW1B–H12	91	251	162	339	OW1B
OW2B–H21	91	221	110	267	O21
OW2B–H21	91	251	143	328	OW2B
OW2B–H22	91	197	172	287	O1

Acknowledgement

The authors thank Mr. *Dominik Saladin*, Albert-Ludwigs-Universität Freiburg, for recording the vibrational spectra and *Prof. Dr. Harald Hillebrecht*, Institut für Anorganische und Analytische Chemie, Albert-Ludwigs-Universität Freiburg, for generous support. Financial support by the *Fonds der Chemischen Industrie* (H. A. H.: Liebig Habilitationsstipendium, K. K.: Doktorandenstipendium) is gratefully acknowledged.

References

[1] a) T. Ben Chaabane, L. Smiri, A. Bulou, *Solid State Sci.* **2004**, *6*, 197; b) H. A. Höppe, M. Daub, O. Oeckler, *Solid State Sci.* **2009**, *11*, 1484.
[2] H. Worzala, *personal communication* to the PDF (data set [43–517]).
[3] a) H. A. Höppe, *Angew. Chem. Int. Ed.* **2009**, *48*, 3572; b) T. Jüstel, H. Nikol, C. Ronda, *Angew. Chem. Int. Ed.* **1998**, *37*, 3084.
[4] M. Schneider, K.-H. Jost, *Z. Anorg. Allg. Chem.* **1983**, *500*, 117.
[5] A. Durif, M. T. Averbuch-Pouchot, *Acta Crystallogr., Sect. C* **1986**, *42*, 927.
[6] T. Schleid, *Z. Anorg. Allg. Chem.* **1999**, *625*, 1700.
[7] S. W. Peterson, V. N. Sadana, W. L. Korst, *J. Phys. Paris* **1964**, *25*, 451.
[8] a) H. A. Höppe, *Z. Anorg. Allg. Chem.* **2005**, *631*, 1272; b) H. A. Höppe, *Solid State Sci.* **2005**, *7*, 1209; c) H. A. Höppe, S. J. Sedlmaier, *Inorg. Chem.* **2007**, *46*, 3468; d) H. A. Höppe, *J. Solid State Chem.* **2009**, *182*, 1786; e) H. A. Höppe, J. M. U. Panzer, *Eur. J. Inorg. Chem.* **2009**, 3127.
[9] T. Balic-Zunic, E. Makovicky, *Acta Crystallogr., Sect. B* **1996**, *52*, 78.
[10] E. Makovicky, T. Balic-Zunic, *Acta Crystallogr., Sect. B* **1998**, *54*, 766.
[11] O. V. Yakubovich, V. S. Urosova, *Kristallografiya* **1997**, *42*, 301.
[12] R. D. Shannon, C. T. Prewitt, *Acta Crystallogr., Sect. B* **1969**, *25*, 925.
[13] a) T. Steiner, *Angew. Chem. Int. Ed.* **2002**, *41*, 48; b) G. A. Jeffrey, *An Introduction to Hydrogen Bonding*, Oxford University Press, Oxford, **1997**.
[14] M. Trojan, P. Sulcova, L. Sykorova, *J. Therm. Anal. Cal.* **2002**, *68*, 75.
[15] J. C. Grenier, C. M. Martin, A. Durif, T. Q. Duc, J. C. Guitel, *Bull. Soc. Fr. Mineral. Cristallogr.* **1967**, *90*, 24.
[16] A. Rulmont, R. Cahay, M. Liegeois-Duyckaerts, P. Tarte, *Eur. J. Solid State Inorg. Chem.* **1991**, *28*, 207.
[17] G. M. Sheldrick, *SHELXTL, V 5.10*, Crystallographic System, Bruker AXS Analytical X–ray Instruments Inc., Madison, **1997**.
[18] a) R. B. von Dreele, A. C. Larson, *General Structure Analysis System (GSAS)*, Los Alamos National Laboratory Report LAUR 86–748, **2000**; b) B. H. Toby, *J. Appl. Crystallogr.* **2001**, *34*, 210.